

where the eigenvector  $|C_{(1)}^i\rangle$  is a solution of the original eigenvalue equation [equation (9)], while  $|C_{(2)}^i\rangle$  is a solution of the equation

$$\mathbf{M}^\dagger |C_{(2)}^i\rangle = 2k\gamma^{i'} |C_{(2)}^i\rangle \quad (\text{A3})$$

or equivalently

$$\langle C_{(2)}^i | \mathbf{M} = 2k\gamma^{i'*} \langle C_{(2)}^i | \quad (\text{A4})$$

where  $\mathbf{M}^\dagger$  denotes the adjoint matrix of  $\mathbf{M}$  and  $\gamma^{i'*} = \gamma^i$ .

Utilizing (A2), we obtain

$$c^i = \langle C_{(2)}^i |_0 / \langle C_{(2)}^i | C_{(1)}^i \rangle \quad (\text{A5})$$

where  $\langle C_{(2)}^i |_0$  is the 0 component of the Bloch-wave eigenvector  $\langle C_{(2)}^i |$ .

By substituting such generalized excitation coefficients into the intensity expression [equation (7)] and neglecting the coupling terms,  $ij$ , the contrast profiles along sections *A* and *B* in Fig. 3 for GaSb have been calculated. The results are shown in Fig. 5.

#### References

- DAVID, M., GEVERS, R. & STUMPP, H. (1985). *Acta Cryst.* **A41**, 204–206.
- DOYLE, P. A. & TURNER, P. S. (1968). *Acta Cryst.* **A24**, 390–397.
- FUJIMOTO, F. (1959). *J. Phys. Soc. Jpn*, **14**, 1558–1568.
- GOODMAN, P. (1975). *Acta Cryst.* **31**, 804–810.
- GOODMAN, P. & LEHMPFUHL, G. (1968). *Acta Cryst.* **A24**, 339–347.
- GRADSHTEYN, I. S. & RYZHIK, I. M. (1980). *Tables of Integrals, Series and Products*. New York: Academic Press.
- HALL, C. R. & HIRSCH, P. B. (1965). *Proc. R. Soc. London Ser. A*, **286**, 158–177.
- HØIER, R. & MARTHINSEN, K. (1986). *Proc. XIth Int. Congr. on Electron Microscopy*, Kyoto, pp. 757–758.
- HUMPHREYS, C. J. (1979). *Rep. Prog. Phys.* **42**, 1825–1887.
- International Tables for X-ray Crystallography* (1962). Vol. III. Birmingham: Kynoch Press. (Present distributor Kluwer Academic Publishers, Dordrecht.)
- KOHRA, K. (1954). *J. Phys. Soc. Jpn*, **9**, 690–701.
- MARTHINSEN, K. (1986). Dr. ing. thesis. Univ. of Trondheim-NTH, Norway.
- MARTHINSEN, K., ANISDAHL, L. & HØIER, R. (1987). *Electron Microscopy and Analysis 1987*, edited by L. M. BROWN, pp. 143–146. Bristol: Institute of Physics.
- MARTHINSEN, K. & HØIER, R. (1986a). *Proc. XIth Int. Congr. on Electron Microscopy*, Kyoto, Japan, pp. 759–760.
- MARTHINSEN, K. & HØIER, R. (1986b). *Acta Cryst.* **A42**, 484–492.
- MARTHINSEN, K. & HØIER, R. (1988). *Acta Cryst.* **A44**, 693–700.
- MIYAKE, S. & UYEDA, R. (1950). *Acta Cryst.* **3**, 314.
- MIYAKE, S. & UYEDA, R. (1955). *Acta Cryst.* **8**, 335–342.
- PETERS, G. & WILKINSON, J. H. (1970). *Numer. Math.* **16**, 181–204.
- REIMER, L., BADDE, H. G., SEIDEL, H. & BÜHRING, W. (1971). *Z. Angew. Phys.* **31**, 145–151.
- SPENCER, J. P. & HUMPHREYS, C. J. (1980). *Philos. Mag.* **A42**, 433–451.
- SPENCER, J. P., HUMPHREYS, C. J. & HIRSCH, P. B. (1972). *Philos. Mag.* **26**, 193–213.
- STEEDS, J. W., TATLOCK, G. J. & HAMPSON, J. (1973). *Nature (London)*, **241**, 435–439.
- STEEDS, J. W. & VINCENT, R. (1983). *J. Appl. Cryst.* **16**, 317–324.
- THIESSEN, P. A. & MOLIÈRE, K. (1939). *Ann. Phys. (Leipzig)*, **34**, 449–460.
- WILKINSON, J. H. & REINSCH, C. (1971). *Handbook of Automatic Computation*. Vol. II, *Linear Algebra*. Berlin: Springer-Verlag.
- YAMAMOTO, T., MORI, M. & ISHIDA, Y. (1978). *Philos. Mag.* **A38**, 439–461.

*Acta Cryst.* (1988). **A44**, 707–714

## Penrose Patterns and Related Structures. II. Decagonal Quasicrystals

BY AKIJI YAMAMOTO\*

*National Institute for Research in Inorganic Materials, Sakura-mura, Niihari-gun, Ibaraki 305, Japan*

AND K. N. ISHIHARA

*Department of Metal Science and Technology, Kyoto University, Sakyo-ku, Kyoto 606, Japan*

(Received 27 October 1987; accepted 28 April 1988)

#### Abstract

Structural relations of the two decagonal phases in Al–Mn and Al–Fe alloys with the Penrose pattern are discussed based on structure-factor calculations and symmetry considerations. The electron diffraction

patterns are explained by models with layer structures which consist of the stacking of four kinds of layers constructing the Penrose pattern. Al–Mn has six layers within a period along the tenfold axis while Al–Fe includes eight. A projection along the axis shows the Penrose pattern in both models. The symmetries of Al–Mn and Al–Fe are expressed by the five-dimensional superspace groups  $P10_5/mmc$  and  $P10_5mc$ . These give the observed systematic extinction rules. In Al–Fe, an additional extinction rule due

\* This work was performed partly while on leave as a visiting member of the Institute of Crystallography, University of Lausanne, Switzerland.

to the symmetry element of the superspace groupoid exists.

### 1. Introduction

In the previous paper of this series (Ishihara & Yamamoto, 1988, hereafter referred to as paper I), the theoretical insight of the generalized Penrose pattern is discussed. Similar considerations are undertaken in this paper to obtain structure models for the decagonal phases of Al-Mn and Al-Fe alloys, which have a tenfold axis and a period along the axis (Bendersky, 1985; Chattopadhyay, Lele, Ranganathan, Subbana & Thangaraj, 1985; Fung, Yang, Zhou, Zhao, Zhan & Shen, 1986). The diffraction patterns of these alloys along the tenfold axis are similar to that of the Penrose pattern (Fig. 1). This implies that their structure consists of several layers (Ho, 1986; Muller, 1987) and the projection along the axis gives the Penrose pattern. The Penrose pattern is divided into four kinds of subpatterns, which come from the four pentagonal atoms in the four-dimensional description of the Penrose pattern described in paper I. Therefore we can construct such a model by considering layers with these patterns. However, we have to consider another possibility because there exists a generalized Penrose pattern with a tenfold axis and this also has a similar diffraction pattern, as stated in paper I. Another point to note is that the decagonal phases show systematic extinction rules, in contrast to the icosahedral Al-Mn quasicrystal. These should be explained by symmetry operations. In order to examine these extinction rules and to construct a model giving diffraction intensities similar to those of the decagonal phases, we extend the symmetry considerations described in paper I to the cases of decagonal Al-Mn and Al-Fe. On the basis of symmetry considerations and structure-factor calculations, simple vertex models for these quasicrystals are proposed and the relations between the two structures

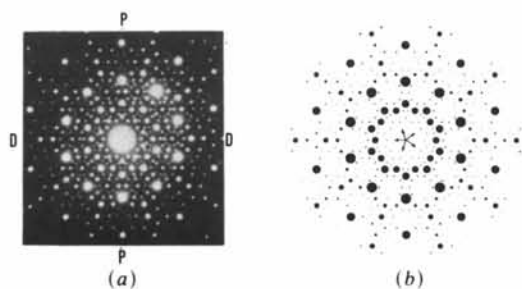


Fig. 1. (a) The electron diffraction pattern of Al-Fe along the tenfold axis (Fung *et al.*, 1986). (b) The calculated diffraction intensity of the Penrose pattern. The radius of the circle is proportional to the structure factor. An isotropic temperature factor of  $1 \text{ \AA}^2$  and the atomic scattering factor of Mn are used. Five arrows show  $\mathbf{p}_i^*$  ( $i = 1, 2, 3, 4$ ) and  $-\sum_{i=1}^4 \mathbf{p}_i^*$ .

and with the Penrose pattern are discussed. The symmetries of these quasicrystals are specified by five-dimensional superspace groups (Janssen, 1986) which explain the systematic extinction rules observed in the diffraction pattern. In Al-Fe an additional extinction rule exists. This is explained by the element of the hull of the groupoid. Such an extinction rule is often observed in polytypes (Verma & Krishna, 1966). We point out that the two models can be regarded as polytypes in the quasicrystal and we discuss their interrelation and symmetry based on groupoid theory (Sadanaga & Ohsumi, 1979). In order to consider realistic models the density of the structure should also be taken into account. Since the present paper considers only vertex models an exact comparison of the density with experimental values is meaningless. Therefore we compare the number densities of the proposed models with that of the three-dimensional Penrose pattern (Elser, 1986). The models give much smaller values than that of the latter. It is shown how we can modify the models to obtain a denser structure leaving the extinction rules and the superspace group unchanged. Finally, we consider other structure models which are related to the generalized Penrose pattern with tenfold axis.

### 2. Extinction rules and superspace groups

The decagonal phases have systematic extinction rules to be explained by the symmetry of the structure. Fig. 2 shows electron diffraction patterns of Al-Mn

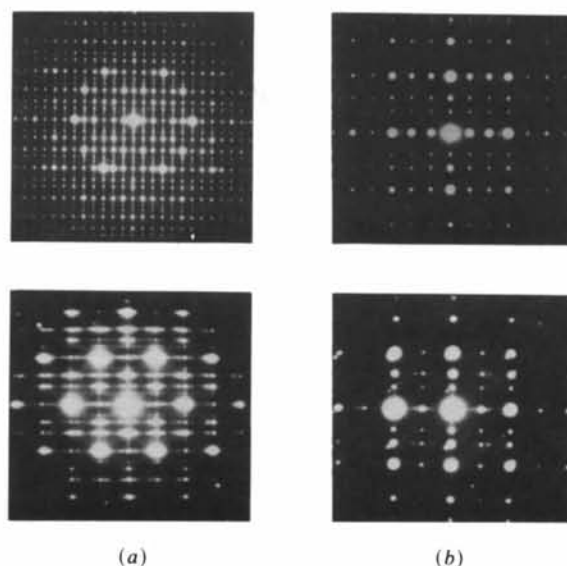


Fig. 2. The electron diffraction patterns of Al-Mn (upper) and Al-Fe (lower) including the tenfold axis along the horizontal line (Fung *et al.*, 1986). (a) and (b) are the sections through  $D$ - $D$  and  $P$ - $P$ , respectively, in Fig. 1(a).  $\mathbf{p}_5^*$  is taken along the horizontal line.

and Al-Fe alloys by Fung *et al.* (1986) which are sections including the tenfold axis (see Fig. 1a). In order to describe the extinction rules we take a decagonal coordinate system. Four vectors  $\mathbf{p}_i^*$  ( $i = 1, 2, 3, 4$ ) are necessary to assign the reflections on planes normal to the tenfold axis (Fig. 1b) and a vector  $\mathbf{p}_5^*$  is parallel to it. (This corresponds to the four-dimensional description of the Penrose pattern.) The five vectors are regarded as the projection of the unit vectors in the five-dimensional reciprocal lattice and the diffraction spots are regarded as the projection of the five-dimensional reciprocal-lattice points onto the three-dimensional space. As with the Penrose pattern, we introduce the unit vectors of the decagonal system  $\mathbf{d}_i^*$  ( $i = 1, 2, \dots, 5$ ) defined by  $\mathbf{d}_i^* = \sum_j \tilde{M}_{ij}^{-1} \mathbf{a}_j$ , where  $\mathbf{a}_i$  ( $i = 1, 2, \dots, 5$ ) are the orthogonal unit vectors with unit length, three of which span the external space and the remaining two the internal space. We take  $\mathbf{a}_1, \mathbf{a}_2, \mathbf{a}_5$  for the basic vectors of the external space and  $\mathbf{a}_3, \mathbf{a}_4$  for those of the internal one. The matrix  $\tilde{M}^{-1}$  is defined by

$$(a^*/\sqrt{5}) \begin{pmatrix} c_1 & s_1 & c_2 & s_2 & 0 \\ c_2 & s_2 & c_4 & s_4 & 0 \\ c_3 & s_3 & c_1 & s_1 & 0 \\ c_4 & s_4 & c_3 & s_3 & 0 \\ 0 & 0 & 0 & 0 & \sqrt{5}c^*/a^* \end{pmatrix}, \quad (1)$$

where  $c_j = \cos(2\pi j/5)$ ,  $s_j = \sin(2\pi j/5)$  ( $j = 1, 2, \dots, 4$ ) and  $a^*$  and  $c^*$  are the reciprocal-lattice constants. The unit vectors  $\mathbf{d}_i$  reciprocal to  $\mathbf{d}_i^*$  are given by  $\mathbf{d}_i = \sum_j M_{ij} \mathbf{a}_j$ .  $M$  is written as

$$(2a/\sqrt{5}) \begin{pmatrix} c_1 - 1 & s_1 & c_2 - 1 & s_2 & 0 \\ c_2 - 1 & s_2 & c_4 - 1 & s_4 & 0 \\ c_3 - 1 & s_3 & c_1 - 1 & s_1 & 0 \\ c_4 - 1 & s_4 & c_3 - 1 & s_3 & 0 \\ 0 & 0 & 0 & 0 & \sqrt{5}c/2a \end{pmatrix}, \quad (2)$$

where  $a = 1/a^*$ ,  $c = 1/c^*$ . The vectors  $\mathbf{p}_i^*$  ( $i = 1, 2, \dots, 5$ ) are regarded as the external components of  $\mathbf{d}_i^*$ , so that these are given by  $\mathbf{p}_i^* = \sum_{j=1}^2 \tilde{M}_{ij}^{-1} \mathbf{a}_j$  ( $i \leq 4$ ) and  $\mathbf{p}_5^* = c^* \mathbf{a}_5$ . The internal components  $\mathbf{q}_i^*$  are  $\sum_{j=3}^4 \tilde{M}_{ij}^{-1} \mathbf{a}_j$  for  $i \leq 4$  and zero for  $i = 5$ . Since the structure has a period along the  $\mathbf{d}_5^*$  axis, the value of  $c^*$  is easily determined from the diffraction pattern. On the other hand,  $a^*$  is not uniquely determined because if unit vectors with some  $a^*$  are available to index all the reflections in the plane other unit vectors with  $\tau a^*$  are also available, where  $\tau$  is the golden mean  $(1 + \sqrt{5})/2$ . This comes from the fact that we can take an infinite number of descriptions which are mutually equivalent. This will be discussed in a separate paper [for the icosahedral quasicrystal see

Yamamoto & Hiraga (1988)]. For convenience we select  $a^*$  so that the diffraction vector  $\mathbf{h}$  is expressed by an integral linear combination of  $\mathbf{d}_i^*$  ( $i = 1, 2, \dots, 5$ ) as  $\mathbf{h} = \sum_{j=0}^5 h_j \mathbf{j}_j^*$  and the strongest reflection on the  $h_1 h_2 h_3 h_4 0$  plane is assigned as 13420. The vectors  $\mathbf{p}_i^*$  ( $i \leq 4$ ) are indicated in Fig. 1(b). In this setting,  $c$  is about  $6a/\sqrt{5}$  for Al-Mn and  $8a/\sqrt{5}$  for Al-Fe. The lattice constant  $a$  of Al-Mn is nearly equal to that of the icosahedral Al-Mn,  $a_0$ , which is about  $4.6 \text{ \AA}$ . [In fact we have  $a = 4.55$  and  $c = 12.44 \text{ \AA}$  in Al-Mn from the X-ray powder pattern (Takeuchi & Kimura, 1986).]

In both cases, reflections with  $h_5$  odd seem to be absent on the plane normal to  $\mathbf{p}_i^*$  ( $i \leq 4$ ) (Fig. 2b), while these reflections appear in Fig. 2(a), which is a plane normal to (b). This implies the existence of a tenfold hyperscrew axis and hyperglide plane normal to the unit vectors  $\mathbf{p}_i^*$  ( $i = 1, 2, 3, 4$ ). In addition another extinction rule appears in both (a) and (b) for Al-Fe: the reflections with  $h_5 = \pm 2, \pm 6, \pm 10$  disappear. It is supposed that this is not due to any symmetry operation. Another point to be considered is the point symmetry of the structures. Al-Mn has point symmetry  $10/mmm$  (Bendersky, 1985) while Al-Fe has  $10mm$  (Fung *et al.*, 1986). This means that Al-Mn has an inversion center but Al-Fe does not. The group  $10/mmm$  is generated by a tenfold axis, a mirror plane including the axis and an inversion. The action of these generators on  $\mathbf{d}_i^*$  ( $i = 1, 2, \dots, 5$ ) is given by a  $5 \times 5$  integral matrix  $\Gamma(R)$ :

$$\Gamma(C_{10}^{-1}) = \begin{pmatrix} 0 & 0 & 0 & -1 & 0 \\ 1 & 1 & 1 & 1 & 0 \\ -1 & 0 & 0 & 0 & 0 \\ 0 & -1 & 0 & 0 & 0 \\ 0 & 0 & 0 & 0 & 1 \end{pmatrix}$$

$$\Gamma(\sigma_v) = \begin{pmatrix} 0 & 0 & 0 & 1 & 0 \\ 0 & 0 & 1 & 0 & 0 \\ 0 & 1 & 0 & 0 & 0 \\ 1 & 0 & 0 & 0 & 0 \\ 0 & 0 & 0 & 0 & 1 \end{pmatrix}$$

$$\Gamma(I) = \begin{pmatrix} -1 & 0 & 0 & 0 & 0 \\ 0 & -1 & 0 & 0 & 0 \\ 0 & 0 & -1 & 0 & 0 \\ 0 & 0 & 0 & -1 & 0 \\ 0 & 0 & 0 & 0 & -1 \end{pmatrix}. \quad (3)$$

The group  $10mm$  is generated by the first two operators. The action on  $\mathbf{a}_i$  is given by a real matrix,

$$\Gamma' = \tilde{M}\tilde{\Gamma}\tilde{M}^{-1};$$

$$\Gamma'(C_{10}^{-1}) = \begin{pmatrix} -c_2 & s_2 & 0 & 0 & 0 \\ -s_2 & -c_2 & 0 & 0 & 0 \\ 0 & 0 & -c_4 & s_4 & 0 \\ 0 & 0 & -s_4 & -c_4 & 0 \\ 0 & 0 & 0 & 0 & 1 \end{pmatrix}$$

$$\Gamma'(\sigma_v) = \begin{pmatrix} 1 & 0 & 0 & 0 & 0 \\ 0 & -1 & 0 & 0 & 0 \\ 0 & 0 & 1 & 0 & 0 \\ 0 & 0 & 0 & -1 & 0 \\ 0 & 0 & 0 & 0 & 1 \end{pmatrix} \quad \Gamma'(I) = \Gamma(I). \quad (4)$$

The reflection condition  $h_5 = 2n$  on the plane mentioned above implies the existence of the hyperscrew axis  $\{C_{10}^{-1}|0000\frac{1}{2}\}$  and hyperglide plane  $\{\sigma_d|0000\frac{1}{2}\}$ . ( $\sigma_d = \sigma_v C_{10}^{-1}$ . We employ decagonal coordinates for the translation vector.) Taking into account these and the point symmetries we have the superspace groups written as  $P10_5/mmc$  for Al-Mn and  $P10_5mc$  for Al-Fe, where the first letter gives the Bravais type, as in the usual symbol;  $P$  denotes the primitive lattice. On the basis of these symmetry operators and the diffraction patterns we construct models for these quasicrystals.

### 3. Structure models

The diffraction patterns of Al-Mn [Fig. 1A of Bendersky (1985)] and Al-Fe (Fig. 1a) along the tenfold axis are similar to that of the Penrose pattern shown in Fig. 1(b). Therefore we first consider a model related to the Penrose pattern. The lattice constants  $a$  and  $c$  imply that Al-Mn has six layers and Al-Fe

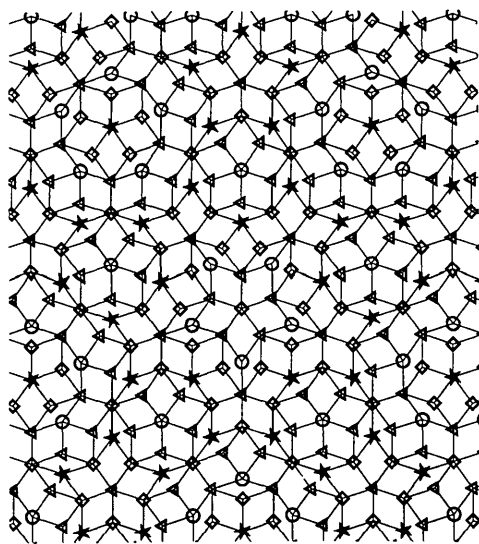


Fig. 3. Distribution of the A, B, C, D atoms in the Penrose pattern (denoted respectively by a circle, triangle, square and star).

eight layers within the period. We consider the four layers obtained from the four pentagonal 'atoms' described in paper I which construct the Penrose pattern. Fig. 3 shows the distribution of the four atoms in the Penrose pattern. In this case the edge length of the rhombus is  $2a/\sqrt{5}$ . The model of the decagonal crystal is given by considering the four layers consisting of each atom. The models are described in the five-dimensional space. The four atoms are continuous within the pentagonal areas in the internal space which are defined by

$$V_\nu = \left\{ \sum_{j=0}^4 \lambda_j \mathbf{e}_{2j} \mid 0 \leq \lambda_j < 1, \sum_{j=0}^4 \lambda_j = \nu \right\} \quad (5)$$

where  $\mathbf{e}_j = (2a/\sqrt{5})[\cos(2\pi j/5)\mathbf{a}_3 + \sin(2\pi j/5)\mathbf{a}_4]$  and  $\nu$  is the index for the atoms which take the values one to four. The shape of  $V_\nu$  is shown in Fig. 4(a). The atoms are called A, B, C, D in the order of  $\nu$  and the layers consisting of them are called A, B, C, D layers for convenience. In Al-Mn we stack the layers as *BABCD*C with an interval of  $c/6 \approx a/\sqrt{5}$  along the tenfold axis while in Al-Fe we consider *BABACDCD* stacking with the same interval. The first- and second-nearest-neighbor distances of these structures are  $2a/\sqrt{5}$  and  $a$ , provided that  $c/6 = a/\sqrt{5}$  for Al-Mn or  $c/8 = a/\sqrt{5}$  for Al-Fe. As shown below, these models have the superspace groups mentioned in the previous section and therefore give the observed extinction rules.

When the atoms A, B, C, D are placed at  $-\nu(11110)/5$  we have the Penrose pattern at  $x_5 = 0$  in the external space, where  $(x_1, x_2, x_3, x_4, x_5)$  denote coordinates referred to  $\mathbf{d}_j$  ( $j = 1, 2, \dots, 5$ ). In order to stack these layers, we take  $x_5 = (2j-1)/12$  or  $(2j-1)/16$  for the  $j$ th layer in Al-Mn or Al-Fe. The atomic coordinates of all the atoms,  $-\nu(1111z)/5$  ( $\nu = 1, 2, \dots, 4$ ), are invariant under  $\{C_5^{-1}|00000\}$  and  $\{\sigma_v|00000\}$  since the coordinates transform as  $x'_i = \sum_j \Gamma(R)_{ij} x_j$ . Furthermore, the pentagons are transformed into themselves because the actions of these on  $\mathbf{a}_3, \mathbf{a}_4$  are written as

$$\begin{pmatrix} c_2 & s_2 \\ -s_2 & c_2 \end{pmatrix} \begin{pmatrix} 1 & 0 \\ 0 & -1 \end{pmatrix}; \quad (6)$$

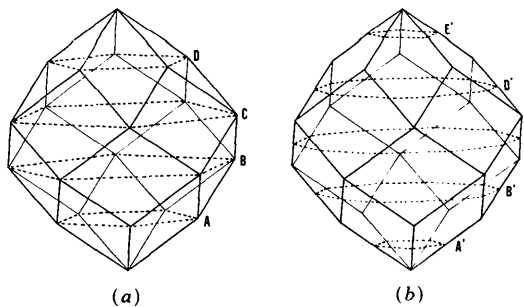


Fig. 4. The atoms constructing (a) the Penrose and (b) generalized Penrose patterns with the tenfold axis. For details see paper I.

these mean the  $4\pi/5$  rotation normal to the pentagon and reflection with respect to the line joining the center and a corner of the pentagon. This indicates that each atom site has site symmetry  $D_5$  and the atom is invariant under this group. The models both have a tenfold hyperscrew axis  $\{C_{10}^{-1}|0000\frac{1}{2}\}$ , by which some atoms are related with the others. The hyperscrew axis transforms  $\pm\nu(1111z)/5$  into  $\pm\nu(-1-1-1-1z')/5$  ( $z'=z+\frac{5}{2}$ ) and rotates each atom by  $7\pi/5$  in the internal space [(see (4)]. Accordingly  $AB$  atoms with  $x_5 < \frac{1}{2}$  in both models are transformed into  $DC$  atoms with  $x_5 > \frac{1}{2}$ . As a result only three atoms are independent in Al-Mn and four in Al-Fe. The symmetry operators  $\{C_{10}^{-1}|0000\frac{1}{2}\}$ ,  $\{\sigma_v|00000\}$  generate, together with the primitive translations, the superspace group  $P10_5mc$ , which includes the hyperglide plane  $\{\sigma_d|0000\frac{1}{2}\}$ . In addition Al-Mn has an inversion center at the origin because the  $B$  atoms at  $x_5 = \frac{1}{12}, \frac{5}{12}$  are transformed into  $C$  atoms at  $x_5 = -\frac{1}{12}, -\frac{5}{12}$  and the  $A$  atom at  $\frac{3}{12}$  into a  $D$  atom at  $-\frac{3}{12}$  by the inversion. The superspace group of Al-Mn is therefore  $P10_5/mmc$  while that of Al-Fe is  $P10_5mc$ .

#### 4. Polytype and groupoid in quasicrystals

The models considered above can be regarded as examples of polytypes in quasicrystals. These have four kinds of layers,  $A, B, C$  and  $D$ . The stacking sequences are  $BABCDC$  in Al-Mn and  $BABACDCD$  in Al-Fe. The latter structure arises from the former by the addition of the  $A$  or  $D$  layer every three layers. These stacking sequences have rules. The  $A$  layer is connected to two layers  $B$  and  $C$  while the  $B$  layer is connected to three layers,  $A, C$  and  $D$ . Similarly the  $C$  layer is joined with  $A, B$  and  $D$  and the  $D$  layer with  $B$  and  $C$ . The characteristic feature is that any layer is not stacked on itself. This is similar to the situation in the SiC polytype. For example the SiC- $6H$  polytype has a stacking of  $ABCACB$  layers along the hexagonal  $c$  axis, where  $A, B, C$  represent the same SiC layer but with Si/C located in different positions. The coordinates of Si are given by  $(0, 0, z), (\frac{1}{3}, \frac{2}{3}, z), (\frac{2}{3}, \frac{1}{3}, z)$  with  $z = n/6$  ( $n = 0, 1, \dots, 5$ ) and for  $C$   $z = (n + \frac{3}{4})/6$  (Verma & Krishna, 1966). Below we discuss peculiar properties in such polytypes.

First we consider the SiC- $6H$  polytype. This is decomposable into six substructures such that every one of these has the same space group and is related to the others by orthogonal transformations. Each substructure consists of one of six layers. The space group of the substructure is  $P6mm$ .  $B, C, A, C, B$  layers are obtained from the first  $A$  layer by  $\{E|\frac{1}{3}, \frac{2}{3}, \frac{1}{6}\}, \{E|\frac{2}{3}, \frac{1}{3}, \frac{1}{6}\}, \{E|0, 0, \frac{1}{2}\}, \{E|\frac{2}{3}, \frac{1}{3}, \frac{2}{3}\}$  and  $\{E|\frac{1}{3}, \frac{2}{3}, \frac{5}{6}\}$ . We write these as  $\mathbf{h}_2, \dots, \mathbf{h}_6$  for simplicity;  $\mathbf{h}_1$  represents the identity operator. The operators  $\mathbf{h}_i$  ( $i = 1, 2, \dots, 6$ ) operate only on the first substructure and superimposes it on the  $i$ th substructure, while  $\mathbf{h}_i^{-1}$  operate on the  $i$ th substructure and superimpose it on the first

one. Then the set of operators which transforms a substructure into another substructure or into itself forms a groupoid (Sadanaga & Ohsumi, 1979). The groupoid  $\mathbf{T}$  is given by  $\{\mathbf{h}_i\mathbf{G}\mathbf{h}_j^{-1} | \mathbf{h}_i, \mathbf{h}_j \in \mathbf{H}\}$ , where  $\mathbf{G}$  is the space group of the substructure and  $\mathbf{H}$  is the set of  $\mathbf{h}_i$ . We call  $\mathbf{G}$  the kernel and  $\mathbf{H}$  the hull of the groupoid  $\mathbf{T}$ . The elements in  $\mathbf{h}_i\mathbf{G}\mathbf{h}_j^{-1}$  superimpose the  $j$ th substructure on the  $i$ th one. It should be noted that  $\mathbf{T}$  is not the set of symmetry operators and does not form any group.

Polytypes sometimes show extinction rules which are not interpreted by the space group. This is due to the existence of particular relations between substructures owing to elements of the hull. The  $6H$  polytype has space group  $P6_3mc$  and this gives the reflection condition  $l = 2n$  for  $hkl$ . In addition, the reflections  $hkl$  with  $h - k = 3n$  are absent except when  $l = 6n$ . This is well known as the structural extinction rule (Verma & Krishna, 1966). This can be regarded as the extinction rule due to the elements of the hull as shown below. We write the structure factor with the diffraction vector  $\mathbf{h}$  of the first substructure as  $F_0(\mathbf{h})$ . This is transformed under the orthogonal translation  $\{R|\tau\}$  into  $\exp(2\pi i\mathbf{h} \cdot \tau)F_0(R^{-1}\mathbf{h})$ . In the present case, the hull leaves all the diffraction vectors invariant. The total structure factor is therefore given by

$$\{(1 + \varepsilon_3) + \exp[2\pi i(h - k)/3](\varepsilon_1 + \varepsilon_2) + \exp[2\pi i(k - h)/3](\varepsilon_2 + \varepsilon_4)\}F_0(\mathbf{h}) \quad (7)$$

where  $\varepsilon_n = \exp(\pi inl/3)$ . The factor in braces gives the extinction rules mentioned above, which include the rule due to the space group  $P6_3mc$ . Although the translation components of the hull element do not effect any limitation from the mathematical structure of the groupoid, if they are rational and the hull leaves some reflections invariant, we can expect the extinction rule inferred from the above argument. In the present example, the hull includes only pure translations, so that all reflections are invariant under the operation of the hull. Accordingly the extinction rules for general reflections are obtained. In general the hull includes the rotation (or rotatory inversion) operator. Then the hull may leave reflections on the axis (or plane) invariant. For such reflections we have a factor  $\sum_{i=1}^n \exp(2\pi i \sum_{j=1}^d \mathbf{h}_j \tau_{ij})$  instead of the factor in braces in (7), where  $n$  is the order of the hull,  $d$  the space dimension and  $\tau_{ij}$  is the  $j$ th translation component of the  $i$ th hull element. The factor vanishes for some reflections because the translation components are rational. In particular if the  $\tau_{ij}$  have a small common divisor, as in the above case, we can easily find the extinction rule due to the elements of the hull. The above consideration suggests that some polytypes in the quasicrystals have extinction rules due to the hull of the groupoid and their symmetry is conveniently specified by the superspace groupoid

instead of the superspace group. In fact, this is the case for Al-Fe.

In Al-Fe the reflections with  $h_5 = \pm(2+4n)$  disappear for general reflections. This is considered to be due to the existence of the elements of the hull in the groupoid. In this case *A*, *B*, *C*, *D* layers appear twice as stated above. One of these is related to the other by the operator  $\{E|0000\frac{1}{4}\}$ . Consider two substructures, one of which is obtained from the other by the operator. Then the structure factor is expressed as  $[1 + \exp(\pi i h_5/2)]F_0(\mathbf{h})$  with the structure factor of the substructure  $F_0(\mathbf{h})$ . The factor in braces vanishes when the above rule is fulfilled. In the present case, the substructure consists of the *B*, *A*, *C*, *D* atoms at  $x_5 = \frac{1}{16}, \frac{3}{16}, \frac{9}{16}, \frac{11}{16}$ , the kernel is the superspace group  $P10mc$  and the hull consists of  $\{E|0000\}$  and  $\{E|0000\frac{1}{4}\}$ . If we consider the groupoid, the independent atoms reduce to *B* and *A* atoms at  $x_5 = \frac{1}{16}$  and  $\frac{3}{16}$ .

### 5. Modified models

The models described in § 3 fulfil the symmetry required to explain the extinction rules and have point groups derived from convergent-beam electron diffraction. However, we have to take into account the density given by the models in addition. The density of the quasicrystal is calculated by applying a method developed by Elser (1986). In the present case, the decagonal phases have several atoms in the unit cell, as described in § 3. Since the method is applied only to the simple case where there is one atom in the unit cell, we briefly describe the steps of the calculation for the present case. We calculate first the number density of the vertices in the Penrose pattern. Consider a simple structure in which only one atom is present in the unit cell of the four-dimensional decagonal lattice spanned by  $\mathbf{d}_j$  ( $j \leq 4$ ). We place the atom defined by  $V_0 = \{\sum_{j=1}^4 \lambda_j \mathbf{q}_j | 0 \leq \lambda_j < 1\}$  at each lattice point, where the  $\mathbf{q}_j$  ( $j = 1, 2, 3, 4$ ) are the internal components of  $\mathbf{d}_j$ . As is clear from the definition,  $V_0$  is the projection of the unit cell into the internal space. When the area of  $V_0$  is written as  $\Omega_0$  and the unit-cell volume of the four-dimensional lattice as  $\Omega$ , the number density of the vertices  $\rho_0$  in the external space is given by  $\Omega_0/\Omega$ . In the present case,  $\Omega_0 = 4\tau^3 \sin(\pi/5)a^2$  and  $\Omega$  is given by  $\det M = 4\sqrt{5}a^4$ , so that the number density is given by

$$\rho_0 = \tau^3 \sin(\pi/5)(\sqrt{5}a^2). \quad (8)$$

As is discussed by Elser (1986), the number density  $\rho$  is proportional to the area of atoms spreading in the internal space. Therefore we find  $\rho_\nu = \rho_0 \Omega_\nu / \Omega_0$  ( $\nu = 1, 2, 3, 4$ ) for the density of *A*, *B*, *C*, *D* atoms in the Penrose pattern, where  $\Omega_\nu$  ( $\nu = 1, 2, 3, 4$ ) are the areas of  $V_\nu$  and are given by  $\Omega_1 = \Omega_4 = 2\tau \sin(\pi/5)a^2$ ,

$\Omega_2 = \Omega_3 = \tau^2 \Omega_1$ . From  $\sum_\nu \rho_\nu$ , we have

$$\rho = \tau^2 \sin(\pi/5)a^2 = 1.5388/a^2 \quad (9)$$

for the Penrose pattern. It is remarkable that the figure of 1.5388 is the same as that of the three-dimensional Penrose pattern, where  $\rho = \tau^2 \sin(\pi/5)/a^3 = 1.5388/a^3$  (Elser, 1986).

We turn to the calculation of the number densities of the models described above. In order to compare these with that of the three-dimensional Penrose pattern, we approximate  $c$  with  $6a/\sqrt{5}$  for Al-Mn and with  $8a/\sqrt{5}$  for Al-Fe. Then  $\rho = (5\tau+2) \sin(\pi/5)/(6a^3) = 0.9885/a^3$  for Al-Mn and  $(3\tau+1) \sin(\pi/5)/(4a^3) = 0.8602/a^3$  for Al-Fe. These are much smaller than that for the three-dimensional Penrose pattern. When we place Mn at every vertex of the three-dimensional Penrose pattern we obtain a diffraction pattern similar to that for icosahedral Al-Mn (Duneau & Katz, 1985) and this model gives a reasonable value for the Mn contribution in the density. Therefore it is reasonable to assume that Mn atoms take the vertices described above in the decagonal phases. Since the chemical composition of the decagonal Al-Mn is nearly equal to that of the icosahedral Al-Mn (Suzuki, Ichihara, Kimura & Takeuchi, 1986) the density due to Mn atoms should be almost the same as that of the icosahedral phase. This leads to the requirement that the number density is almost the same as that of the three-dimensional Penrose pattern. The models considered above give unacceptably small densities for both cases. Therefore denser structures giving the observed extinction rules should be considered. Although Al atoms must also be taken into account in a real model, vertex models with reasonable number densities are treated as the zeroth approximation in this paper.

Such models are obtained in the *BABCD*C sequence of Al-Mn and the *BABACD*CD sequence of Al-Fe by replacing *A* and *D* with *A+C* and *D+B*, where *A+C* (*D+B*) means the layer consisting of the *A* and *C* (*D* and *B*) atoms (see Fig. 3). These give nearly the same densities of  $1.4036/a^3$  and  $1.4826/a^3$  for Al-Mn and Al-Fe as that of the three-dimensional Penrose pattern. These structures also have the same superspace group and the same superspace groupoid as those of the original ones, so that the same extinction rules are obtained. The nearest-neighbor distance reduces from  $2a/\sqrt{5}$  in the models discussed in § 3 to  $a/\tau$  because *A* and *C* or *B* and *D* atoms are at the same height along the *c* axis. This is acceptable in crystal chemistry terms as the inter-Mn or inter-Fe distance. In the structure analysis of the decagonal phases, such models are considered to be better than the models described in § 3 as starting models. The coordinates of the independent atoms in the five-dimensional unit cell are given in Table 1.

Table 1. *The atom coordinates of the independent atoms in the modified models for decagonal Al-Mn and Al-Fe*

In the first column *A* and *B* represent the kind of pentagonal atoms which are shown in Fig. 4. The coordinates specify the center of the atoms.

Al-Mn	$x_1$	$x_2$	$x_3$	$x_4$	$x_5$
<i>B</i>	$\frac{1}{12}$	$\frac{1}{12}$	$\frac{1}{12}$	$\frac{1}{12}$	$\frac{1}{12}$
<i>A</i>	$\frac{3}{12}$	$\frac{3}{12}$	$\frac{3}{12}$	$\frac{3}{12}$	$\frac{3}{12}$
<i>C</i>	$\frac{5}{12}$	$\frac{5}{12}$	$\frac{5}{12}$	$\frac{5}{12}$	$\frac{5}{12}$
<i>B</i>	$\frac{1}{12}$	$\frac{1}{12}$	$\frac{1}{12}$	$\frac{1}{12}$	$\frac{1}{12}$
Al-Fe	$x_1$	$x_2$	$x_3$	$x_4$	$x_5$
<i>B</i>	$\frac{1}{16}$	$\frac{1}{16}$	$\frac{1}{16}$	$\frac{1}{16}$	$\frac{1}{16}$
<i>A</i>	$\frac{3}{16}$	$\frac{3}{16}$	$\frac{3}{16}$	$\frac{3}{16}$	$\frac{3}{16}$
<i>C</i>	$\frac{5}{16}$	$\frac{5}{16}$	$\frac{5}{16}$	$\frac{5}{16}$	$\frac{5}{16}$

## 6. Structure factors

The structure factor of the Penrose pattern is derived in paper I. Similar considerations allow a derivation of the structure-factor formula for the decagonal quasicrystal models described in the previous two sections. In the present case we take into account the scattering factor of atoms and the temperature factor. In the modulated and/or quasicrystal structure, the additional Debye-Waller factor due to the phason should be taken into account (Yamamoto, Nakazawa, Kitamura & Morimoto, 1984; Kalugin, Kitayev & Levitov, 1985; Yamamoto & Hiraga, 1988). This is, however, neglected in the present calculation. Then the structure factor is expressed as

$$F_{\mathbf{h}} = \sum_{\mu} \sum_{\{R|\tau\}} f^{\mu}(\mathbf{h}^e) \exp\{-B^{\mu}(\mathbf{h}^e)^2 + 2\pi i \sum_{i=1}^5 h_i [(R\mathbf{x}^{\mu})_i + \tau_i]\} F^{\mu}(R^{-1}\mathbf{h}), \quad (10)$$

where  $\mu$  indicates the index of the independent atoms,  $\{R|\tau\}$  represents the symmetry operator of the superspace group (and the element of the hull mentioned in the previous section for the case of Al-Fe),  $f^{\mu}(\mathbf{h}^e)$  is the atomic scattering factor of the  $\mu$ th atom at the external component  $\mathbf{h}^e$  of the diffraction vector  $\mathbf{h}$ ,  $B^{\mu}$  is the isotropic temperature factor and  $F^{\mu}(\mathbf{h})$  is the Fourier integral of the pentagonal atom spreading in the internal space. An explicit expression for  $F^{\mu}(\mathbf{h})$  is given in paper I. The index  $\mu$  runs over independent atoms and the summation with respect to  $\{R|\tau\}$  is taken over the identity operator  $\{E|00000\}$  and all the symmetry operators which generate new atoms from the independent ones. In Al-Fe the operators combined with these and the element of the hull are also included in the summation. These are  $\{E|00000\}$ ,  $\{C_{10}|0000\frac{1}{2}\}$  for Al-Mn and  $\{E|0000\frac{1}{4}\}$ ,  $\{C_{10}|0000\frac{3}{4}\}$  are added for Al-Fe. Noting that  $(R\mathbf{x}^{\mu})_i$  is given by  $\sum_{j=1}^5 \Gamma(R)_{ij} x_j^{\mu}$  we obtain the extinction rules due to the tenfold hyperscrew axis and hyperglide plane.

From the hyperscrew axis we have the reflection condition  $h_5 = 2n$  for  $0000h_5$  and from the hyperglide plane,  $h_5 = 2n$  for  $h_1h_2h_3h_4h_5$  with  $h_1 + h_2 = h_3 = 2h_4$ . [The rotation matrix of the hyperglide plane  $\Gamma(\sigma_d)$  is given by  $\Gamma(\sigma_v)\Gamma(C_{10}^{-1})$ .] The latter includes the former.

The calculated diffraction patterns for the modified models of Al-Mn and Al-Fe are shown in Fig. 5. Here we have used the atomic scattering factor of Mn and an isotropic temperature factor of  $1 \text{ \AA}^2$  for all atoms in both cases because the difference of the scattering factor in Mn and Fe is negligible in the present rough models. It is clear that the observed extinction rules are reproduced and the diffraction intensity explains the characteristic features of that in Al-Mn and Al-Fe though quantitative comparison is meaningless because the models do not take into account the Al atoms.

## 7. Discussion

As shown in paper I another generalized Penrose pattern with a tenfold axis gives a diffraction pattern similar to that of the Penrose pattern. This has five kinds of layers, *A'*, *B'*, *C'*, *D'*, *E'* which come from the five atoms shown in Fig. 4(b). The *C'* atom has tenfold symmetry while the remaining ones have fivefold symmetry. Taking into account this and the superspace-group symmetry, we can hardly consider the model of Al-Mn with these five layers because it consists of six layers as stated previously. Therefore we consider a model with three layers, *B'*, *C'*, *D'*, which are stacked as *B'C'B'D'C'D'* along the tenfold axis. This has the superspace group  $P10_5/mmc$  as in the previous model. The model by no means gives a generalized Penrose pattern when it is projected along the tenfold axis owing to the lack of *A'* and *E'* layers. Its diffraction pattern is, however, not much different

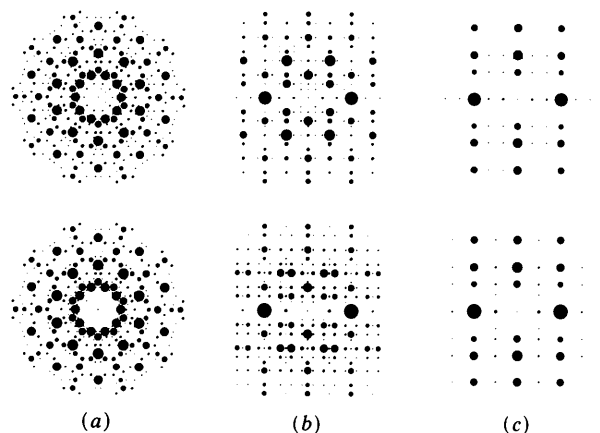


Fig. 5. Calculated diffraction patterns for the modified Al-Mn (upper) and Al-Fe (lower) models. (a) corresponds to Fig. 1 in Bendersky (1986) or Fig. 1(a) of the present paper; (b) and (c) correspond to Figs. 2(a) and (b).

from that of the generalized Penrose pattern because the number density of these atoms are small compared with the others. Similarly we can consider  $B'C'B'C'D'C'D'C'$  stacking for the model of Al-Fe. These models again give a density much smaller than that of the three-dimensional Penrose pattern:  $\rho = 1.0677/a^3$  for Al-Mn and  $1.1488/a^3$  for Al-Fe because  $\Omega_v$  for  $B'$  and  $D'$  is  $(7\tau+1)\sin(\pi/5)a^2/2$  and that for  $C'$  is  $(4\tau+3)\sin(\pi/5)a^2$ . [For  $A'$  and  $E'$  we have  $\Omega_v = \tau\sin(\pi/5)a^2/2$ . This means that two generalized Penrose patterns with tenfold axis have the same point density. Similar considerations show that all the generalized Penrose patterns have the same point density.] It seems difficult to obtain any other stacking sequence giving a reasonable density from these layers. The above consideration suggests that the decagonal phases of Al-Mn and Al-Fe consist of  $A, B, C, D$  layers. It should be noted that if the decagonal phases consist of  $A, B, C, D$  or  $B', C', D'$  layers, the Mackay icosahedron does not appear because this requires a 12-fold vertex. The Mackay icosahedron consisting of 12 Mn and 42 Al is an important building unit of icosahedral Al-Mn (Elsner & Henley, 1985; Guyot & Audier, 1985; Yamamoto & Hiraga, 1988). The  $B'D'D'$  stacking includes tenfold vertices, which provide ten of 12 Mn positions in the Mackay icosahedron. If the Mackay icosahedron is also important in the decagonal phase as a building unit, we have to consider a more complicated model different from the generalized Penrose pattern.

### 8. Concluding remarks

It has been pointed out that extinction rules are observed in the decagonal Al-Mn and Al-Fe quasicrystals. For Al-Mn these are explained by the superspace group  $P10_s/mmc$ . On the other hand, the superspace group of Al-Fe is  $P10_3mc$  but this group explains only part of the rules. An extra extinction rule is due to the groupoid symmetry. Symmetry considerations are important in constructing models for these quasicrystals and are efficient in calculations of the structure factor. Symmetry operations reduce the number of atoms to be considered. The structure

is determined by fixing parameters of independent atoms owing to the symmetry operators. Based on symmetry considerations and structure-factor calculations some structure models have been proposed. The models consist of four kinds of layers which are derived from the Penrose pattern. These give reasonable densities and diffraction patterns characteristic of the decagonal phases. The polytypism in the quasicrystals was discussed with respect to the groupoid symmetry and the structural extinction rules. It was shown that the superspace groupoid plays an important role in describing some quasicrystal symmetry.

The authors thank Dr K. K. Fung, Institute of Physics, Chinese Academy of Sciences, for supplying the electron diffraction patterns of decagonal quasicrystals. One of the authors (AY) acknowledges discussions with Professor G. Chapuis, University of Lausanne. This work is indebted to the Swiss National Science Foundation.

### References

- BENDERSKY, L. (1985). *Phys. Rev. Lett.* **55**, 1461-1463.  
 CHATTOPADHYAY, K., LELE, S., RANGANATHEN, S., SUBBANA, G. N. & THANGARAJ, N. (1985). *Current Sci.* **54**, 895-903.  
 DUNEAU, M. & KATZ, A. (1985). *Phys. Rev. Lett.* **54**, 2688-2691.  
 ELSNER, V. (1986). *Acta Cryst.* **A42**, 36-43.  
 ELSNER, V. & HENLEY, C. L. (1985). *Phys. Rev. Lett.* **55**, 2883-2887.  
 FUNG, K. K., YANG, C. Y., ZHOU, Y. Q., ZHAO, J. G., ZHAN, W. S. & SHEN, B. G. (1986). *Phys. Rev. Lett.* **56**, 2060-2063.  
 GUYOT, P. & AUDIER, M. (1985). *Philos. Mag.* **B52**, L15-L19.  
 HO, T. L. (1986). *Phys. Rev. Lett.* **56**, 468-471.  
 ISHIHARA, K. N. & YAMAMOTO, A. (1988). *Acta Cryst.* **A44**, 508-516.  
 JANSSEN, T. (1986). *Acta Cryst.* **A42**, 261-271.  
 KALUGIN, P. A., KITAYEV, A. Y. & LEVITOV, L. S. (1985). *J. Phys. (Paris) Lett.* **46**, L601-L607.  
 MULLER, S. (1987). *Europhys. Lett.* **3**, 587-592.  
 SADANAGA, R. & OHSUMI, K. (1979). *Acta Cryst.* **A35**, 115-122.  
 SUZUKI, K., ICHIHARA, M., KIMURA, K. & TAKEUCHI, S. (1986). *Proc. XIth Int. Congr. on Electron Microscopy, Kyoto, Japan*, pp. 1529-1530.  
 TAKEUCHI, S. & KIMURA, K. (1986). *J. Phys. Soc. Jpn.* **56**, 982-988.  
 VERMA, A. R. & KRISHNA, P. (1966). *Polymorphism and Polytypism in Crystals*. New York: John Wiley.  
 YAMAMOTO, A., NAKAZAWA, H., KITAMURA, M. & MORIMOTO, N. (1984). *Acta Cryst.* **B40**, 228-237.  
 YAMAMOTO, A. & HIRAGA, K. (1988). Submitted to *Phys. Rev. B*.